BILINGUAL PUBLISHING GROUP

Journal of Atmospheric Science Research

https://journals.bilpubgroup.com/index.php/jasr

ARTICLE

A Formation of Atmospheric Aerosol Particles Due to Gas-to-Particle Conversion in Dark Conditions and the Particles' Evolution in Large (3200 m^3) Isolated Volume

Sergey Dubtsov [1] **, *Vladimir Ivanov*** [2] **, *Oleg Ozols*** [2] **, *Alexei Palei*** [3] **, *Yuri Pisanko*** [3,4*] **, *Nikolai Romanov*** [2] **, *Dzhalil Sachibgareev*** [2] **, *Marina Vasilyeva*** [5]

[1] *Laboratory of Nanoparticles, Voevodsky Institute of Chemical Kinetics and Combustion SB RAS, Institutskaya st.3, Novosibirsk 630090, Russia*

[2] *Department of Atmospheric Modeling, RPA "Typhoon", Pobeda st.4, Obninsk 249038, Kaluga Region, Russia*

[3] *Department of Geoeffective Radiation, Fedorov Institute of Applied Geophysics, Rostokinskaya st.9, Moscow 129128, Russia*

[4] *Ocean's Thermo-Hydromechanics Chair, Moscow Institute of Physics and Technology (National Research University), Institutsky Lane 9, Dolgoprudny 141701, Moscow Region, Russia*

[5] *Guarding and Management Chair, Russian University of Transport (MIIT), Obraztsova st.9, Moscow 127994, GSP-4, Russia*

ABSTRACT

We observe the formation of the particles due to gas-to-particle conversion in complete darkness and UV irradiation absence. The study was carried out in the Large Aerosol Chamber (LAC) of Research and Production Association (RPA) "Typhoon" having 3200 m^3 volume. Because of the large size of the LAC, it is possible to exclude the boundary conditions influence by chamber walls and the equipment inside the LAC on the processes under study. The LAC has two (external and internal) High Efficiency Particulate Air (HEPA) 13 class filters installed at the entrance and inside it. First, we fill out

*CORRESPONDING AUTHOR:

Yuri Pisanko, Department of geoeffective radiation, Fedorov Institute of Applied Geophysics, Rostokinskaya st.9, Moscow 129128, Russia; Email: pisanko@ipg.geospace.ru

ARTICLE INFO

Received: 28 May 2024 | Revised: 25 July 2024 | Accepted: 11 September 2024 | Published Online: 11 October 2024
DOI: https://doi.org/10.30564/jasr.v7i4.6738

CITATION

Dubtsov, S., Ivanov, V., Ozols, O., et al., 2024. A Formation of Atmospheric Aerosol Particles Due to Gas-to-Particle Conversion in Dark Conditions and the Particles' Evolution in Large (3200 m^3) Isolated Volume. Journal of Atmospheric Science Research. 7(4): 1–12. DOI: https://doi.org/10.30564/jasr.v7i4.6738

the LAC of the atmospheric air and close it. After that, we purify the air inside the LAC by the internal filter. The number concentration of particle sizes above 15 nm decreases down to 50 particles per cm^3. However, after a while, we observe increasing the particle number concentration by more than two orders of magnitude. We suppose that new formed particles due to gas-to-particle conversion were detected. We again purify the air inside the LAC by the internal filter. The particle number concentration decreased down to 10–20 particles per cm^3 and remained at this low value for more than 300 hours. Our experiments indicate the necessity to use the two-stage procedure for cleaning working areas, with a time gap enabling gaseous precursors to form new particles, removable by HEPA 13 filter. Regularities of the growth of the newly formed particles from 15 nm size to cloud condensation nuclei characteristic size under controlled conditions were investigated. The observed regularities could contribute to understanding the atmospheric aerosol formation process responsible for cloudiness and precipitations.

Keywords: Aerosol Evolution; New Particle Formation; Big Aerosol Chamber

1. Introduction

The atmospheric aerosol is essential in a modern climate state[1]: the formation of cloudiness looks impossible without its participation. After[2, 3], it was considered[4] that hydroscopically active atmospheric particles were formed from secondary aerosols by nucleating so-called conversion gases in the atmospheric air. The secondary aerosols formed due to the gas-particle conversion result from Brownian coagulation grow to a size of 100–300 nm and could be suppliers of condensation nuclei for the nucleation of cloud droplets. According to[5] the new particle formation events one can observe practically in all atmospheric conditions. Moreover, depending on meteorological and geographical conditions, their growth rate varies by several orders of magnitude; the aerosol spectra collected on 24 European stations were presented in the studies of Asmi et al.[6].

Currently, the problem of the newly-formed particles due to gas-to-particle conversion aerosol spectra evolution can be solved in two interconnected (parallel) directions. The first one is to conduct studies of the dependence of secondary aerosol formation in natural conditions, which differ for anthropogenic and natural sources of conversion gases. In Finland, in 1962, a station for study the ecosystem-atmospheric relationships for boreal coniferous forest (station for measuring ecosystem-atmospheric relation SMEAR II) was established[7] to clarify the role of the natural sources of conversion gases. That forest covers 8% of the Earth's surface and stores about 10% of the total carbon in the terrestrial ecosystem. The previous studies of Dal Maso et al.[8] recorded an average explosive occurrence of new particles in 24% of cases at this station between 1996 and 2003. Similar processes were observed at other Northern field stations[9]. Therefore, one can conclude that boreal coniferous forest, which releases isoprene and terpenes, participates in forming the aerosol component in the European region. The authors of the paper Drofa A.S. et al.[10] supposed the predominant role of solar radiation in the new particle formation mechanism from conversion gases and also the possible role of ions.

However, a detailed study of the secondary aerosol formation mechanism in natural conditions is not possible due to the variability of these conditions. Therefore, the other natural method to study such processes is their reproduction in laboratory (chamber) conditions.

In a chamber, one can measure and investigate aerosol formation under controlled and repeatedly reproducible conditions using various accurate laboratory instruments. However, this raises the question of taking into account the chamber walls' influence. Because of the small volume of a chamber, the process of particles deposition on their walls can be a significant obstacle. The attempts to make low-cost chamber volume up to 240 m^3 from steel frames covered with fluoroplastic film encountered the strong interaction of the material with organic gases. Influence of ozone and OH radical on new particle formation from terpenes emissions of pine trees grown for these purposes were observed[11–19] in a similar chamber with a volume of 6 m^3, specially made for operation under natural conditions. Due to the small volume of the chamber, the duration of the measurements was only two hours. The amorphous nature of organic aerosol particles was revealed[20] in this chamber.

Cosmic Leaving Outdoor Droplets (CLOUD) camera is constructed in CERN (Switzerland) with Proton Synchrotron with a volume of 26.1 m^3 and has walls from electro-polished stainless steel. The air in the chamber is produced by the evaporation of liquid nitrogen and oxygen [21, 22]. In this chamber, a temperature from 183 K to 300 K can be controlled with an accuracy of 0.01 K and may be elevated up to 373 K for cleaning the walls from possible contaminants. In addition, a calibrated amount of conversion gases SO_2, NH_3, and other organic and inorganic gas components may be added to the chamber. It is possible to regulate ionic compounds in the chamber from zero concentrations by creating a constant electric field up to a natural background from galactic cosmic rays and additional ionization of the air from the Proton Synchrotron π+-meson beam and solar radiation as well. Unfortunately, the studied process duration in this chamber is limited to five hours due to the wall influence, and this chamber does not provide the injection of outdoor air.

Studying secondary aerosol formation processes in various outdoor conditions shows the diversity of the conversion gases composition. The published paper of Pöschl et al. [23] showed that in the Amazon region with no anthropogenic pollution, the primary source of the condensing material was organic compounds emitted by plants. Nevertheless, the ratio of biogenic and anthropogenic sources of these precursors in the atmosphere is still poorly understood [24, 25]. Therefore, it is essential to study the formation and evolution of secondary aerosols in outdoor air in much larger volumes, where the wall influence can be minimized. For this purpose one can use the 3200 m^3 Large Aerosol Chamber (LAC) available at the Research and Production Association "Typhoon", filled with external air. The LAC is situated in Obninsk (54o north latitude, 35o east longitude), Kaluga region, central Russia. The most part of the Kaluga region is a plain. Forests occupy 45.2% of the Kaluga region territory. The trees in these forests are fir, pine, birch, asp, lime, and oak. At present, the chamber is equipped with two (external and internal) High Efficiency Particulate Air (HEPA) 13 class filters [26]. This makes possible to reach almost zero aerosol concentration in the LAC for a very long period (more than two weeks). It means that neither the chamber walls nor equipment installed inside the chamber produce aerosol particles.

So, the large chamber volume allows eliminating wall influence on particle sedimentation: in the LAC, it is possible to study processes of atmospheric aerosol formation and further evolution in close to natural conditions—the nucleation formation processes of secondary aerosols from the introduced gas impurities can be experimentally studied with a trace of their evolutionary development and the evolution of atmospheric aerosol in the absence of the source of a secondary aerosol. The almost zero aerosol production by chamber walls and equipment inside as well as the ability to perform laboratory experiments during weeks is a novelty of our approach.

The purpose of the paper is the experimental confirmation of the generation of new aerosol particles from atmospheric components inside the Large Aerosol Chamber.

2. Experiments

2.1. The Large Aerosol Chamber (LAC) Device Description

The largest cloud investigation chamber constructed in 1954 in Texas, the USA [27] has a spherical shape with an internal diameter of 60 feet (volume 3200 m^3) with a steel wall thickness of one inch. The first studies of aerosol concentration dependence on atmospheric aero-ion concentration one conducted in this chamber [28]. In Russia, a similar cylinder chamber with the same volume was built in Obninsk in 1964 as an integral part of the complex facilities of RPA "Typhoon", designed for cloud and meteorological proposes investigation.

The LAC design and its thermodynamic characteristics are described in the paper of Romanov et al. [29]. The chamber represents a hermetic steel cylinder 15 meters in diameter and 18 meters height, the inner surface of which is painted with ship paint. Outside, the chamber is covered with a shell of heat-insulating material 10 cm thick and a decorative fence hiding its unaesthetic forms. The entire construction of the chamber is in the building and is surrounded by adjacent working premises isolated from each other. The chamber wall thickness is 6 mm allows it to withstand excess pressure up to 0.07 MPa. The water-packed ring compressor produces this pressure in about 50 minutes. Reducing this pressure through a system of seven valves allows simulating the cloud cumulus formation with an adjustable rate of air mass rise. Filling the chamber with outside air one car-

ried out by sucking it through the premise adjacent windows and the inlet using an exhaust fan located in the upper part of the chamber through a valve with a nominal diameter DN = 800 mm. In this case, the complete replacement of the internal air by the external environment takes place over approximately 0.5 hours. Since 2014, one has been cleaning aerosols of air drawn in through the chamber by installing a HEPA 13 class air filter at the entrance to the vestibule. The company "AeroFilter" LLC (operating in Obninsk), which manufactured the filter, guarantees the absence of aerosols larger than 15 nm after the filtration. The dimensions of the filter are equal to the entrance vestibule dimensions. At the same time, the time for replacing air in the chamber with the air cleared of aerosol increases up to about one hour. A similar air filter with its fan is also available inside the chamber. During its operation, approximately two hours, the aerosol concentration inside the LAC decreases by about three orders of magnitude. The photo of the chamber internal view is presented in **Figure 1**.

Figure 1. Photo of the LAC interior view. 1—entrance portal with size 60×160 cm^2; 2—rail for mounting the tested equipment; 3—the hanging platform with temperature sensors (for measuring dry and wet air), optical depth sensor with 4 m optical path and a photoelectric sensor for measurement of cloud droplets size; 4—inner HEPA filter.

The size dimensions of the HEPA 13 filter (position 4 in the picture) are equal to the entrance vestibule dimensions (position 1). The second same air filter without a fan is outside the chamber. All lanterns located on the chamber walls for commissioning are turned off during experiments. In 2014, the chamber was equipped with SMPS Scanning Monitor Particle Sizer model 3936L88-N (TSI Inc.). The experiment size range is from 15 to 1000 nm with 115 measurement channels. For sampling air from the LAC, we use a 2 m long zinc-coated steel tube with an inner diameter of 18 mm. A similar tube for outdoor air sampling goes through a window near SMPS. The influence of these tubes on the measured particle size was considered during the data processing according to the SMPS manual.

2.2. LAC Radiation and Ionization State

Ions in the air can play a significant role in secondary aerosol nucleation, so it is essential to know their concentration to study the secondary aerosol formation processes. The speed of secondary aerosol formation cannot exceed the ion pairs (i.p.) formation speed under the influence of ionizing radiation[30]. For the chamber in CERN, this speed under the influence of natural radiation is 2 $i.p.\ per\ cm^3\ per\ sec.$ To determine this characteristic, we carried out several 7–10 days measurements during the second half of 2019 and January 2020. We measured the dose rate (DR) in the LAC with a gamma radiometer using Geiger-Muller counters (model БДКГ-1). The measured dose (*DR*) was 8–10 *μR per h*. Hence, under the *DR* = 1 *R per h* $i.p = 2.06 \cdot 10^9 i.p.\ per\ cm^3\ per\ sec.$ So we obtained the ionization rate in the chamber at normal pressure $\approx 5\ i.p.\ per\ cm^3\ per\ sec.$ DR measurements near indication the LAC and outside the building usually exceed the chamber by approximately 20%. To us such a slight decrease in DR in the chamber is because the muons, responsible for the ionization of nitrogen and oxygen molecules in the lower atmosphere, are highly penetrating, and the chamber walls cannot filter them so that muons can ionize gas molecules inside the chamber. We did not carry out a detailed study of the air ion formation in the LAC because it requires long-term experiments with various parameters. However, our preliminary conclusion follows from several conducted experiments that the resulting ion concentration in the chamber mainly depends on the aerosol concentration and establishes within a few hours. So for a single experiment with the aerosol concentration changing from $7 \cdot 10^3 cm^{-3}$ to $50\ cm^{-3}$ using internal HEPA 13 filter the light ion concentration with mobility $\geq 0.4\ cm^2\ per\ V\ per\ sec$ is for positive ions at a level from $4 \cdot 10^2 cm^{-3}$ to $4 \cdot 10^3 cm^{-3}$ correspondingly.

2.3. Forming and Nucleation Aerosol Evolution Process

According to the coagulation and sedimentation laws, the rate of number particle concentration *N(t)* is proportional to the first and the second degree of the coagulation *K* and sedimentation *D* factors correspondingly[31–34]:

$$\frac{dN}{dt} = -KN^2 - DN \tag{1}$$

with the solution:

$$N(t) = \frac{N(t_1)\, exp\left((t_1 - t)\cdot D\right)}{1 + KN(t_1)/D \cdot (1 - exp\left((t_1 - t)\cdot D\right))} \tag{2}$$

where t_1 is the time moment when the LAC is hermetically closed after it has been filled an outdoor air and purified by the external HEPA 13 filter. The Equation (2) could have an additional constant term on the right-hand side, defining the particle inflow from an extraneous source[35], but we have no an extraneous source and, hence, no constant term.

For $D \to 0$

$$N(t) = \frac{N(t_1)\, exp\left((t_1 - t)\cdot D\right)}{[1 + N(t_1)(t - t_1)\cdot K]} \tag{3}$$

Note that Equations (2) and (3) imply that factors *K* and *D* do not depend on the particle size. Usually, one can use them for $t \geq t_1$ to predict *N(t),* and we use them for the early stages $t < t_1$ of the coagulation spectra formation when it is impossible to measure the concentration with the instruments. The value t_0 is defined when the denominator of Equation (3) is zero:

$$t_0 = t_1 - \frac{1}{K \cdot N(t_1)} \tag{4}$$

To compare with the experiment, we use normalized distribution function $f(d) = n(d)/N(t)$ with *n(d)* from[4]. The Equation (5) represents moments *l(n)*, taking into account *l(0) = 1* and median diameter d_m = *l(1)*.

$$l(n) = \int_0^\infty f(d)\cdot d^n dd \tag{5}$$

Equations (6)–(8) define other dimensionless parameters:

relative count standard deviation

$$\sigma_c{}^2 = \frac{\int_0^\infty f(d)\cdot (d - d_m)^2 dd}{d_m^2} \tag{6}$$

asymmetry factor

$$kas = \frac{\int_0^\infty f(d)\cdot (d - d_m)^3 dd}{\left[\int_0^\infty f(d)\cdot (d - d_m)^2 dd\right]^{3/2}} \tag{7}$$

relative asymmetry

$$ras = kas/\sigma_c{}^2 \tag{8}$$

We will consider the simplest two-parameter distributions for the experimental data approximation: the gamma (*g*), the lognormal (*ln*), and the Smirnov (*Sm*) which are defining by *kas* and σ_c values. From the following relationships between *ras* and σ_c[36, 37]:

$$ras(g) = 2; ras(ln) = 3 + \sigma_c^2; ras(Sm) = 4/(1 - \sigma_c^2) \tag{9}$$

One can see that the gamma distribution (defined by the Equation (10)) has the minor relative asymmetry *ras = 2*.

$$f_\gamma(u)\, du = \frac{\mu^\mu}{\Gamma(\mu)} u^{\mu-1}\cdot exp(-\mu\cdot u) du \tag{10}$$

Here, $u = d/d_m$; $\mu = 1/\sigma_c{}^2$.

If $ras > 2$, one can use a sum of the other distributions having factors defined by (9).

We calculate dependency *m(t)* with the same factors *K* and *D* by the following equation.

$$m(t) = m(t_0)\frac{N_2(t)}{N_3(t)} \tag{11}$$

Here, $m(t_0 = 20ours) = 0.44\mu gperm^3$. *$N_2$(t)* is calculated by equation (2) with reference point $N(t = 20) = 4200cm^{-3}$ (with $K = 9.05\cdot 10^{-6}\left(cm^3perours\right) \equiv 2.5\cdot 10^{-15}(m^3persec)$, and $D = 2.6\cdot 10^{-3}\left(ours^{-1}\right) \equiv 7.2\cdot 10^{-7}\left(sec^{-1}\right)$). *$N_3$(t)* is obtained by equation (3) with the same factors *K* and *N*(*t* = 20 hours).

In case of time dependence of *K(t)* and *D(t)* we will use the following expression:

$$m(t) = \frac{m(t_1)}{[1 + \alpha(t - t_1)]^{6/5}} \tag{12}$$

where t_1 is the time moment when the LAC is hermetically closed after it has been filled an outdoor air and purified by the external HEPA 13 filter.

3. Results

In this section, we present the results which testify to the experimental confirmation of new particle formation from atmospheric components inside the LAC.

3.1. Heat Exchange and Air Motions in the LAC; Procedure of Experiments with Particle Number Evolution

The integral heat capacity of the walls and structures adjacent to them exceeds the integrated heat capacity of air by 10–15 times. When simulating the cumulus cloud formation by reducing the previously created overpressure, the temperature difference between the wall and air usually varies from plus 5 to minus 10 K. The heat transfer consists of ¾ with IR emission exchange of chamber walls with water vapors and ¼ convective heat exchanges [29]. More detailed study indicated that the convective heat exchange occurs in ascending (descending) airflow in a 5–10 cm thick layer close by vertical walls and horizontal movements near the floor [38]: as a result, a homogeneous temperature (the accuracy 0.1 K) is established in the chamber's entire horizontal layer (except for the regions near walls).

In stationary conditions without excess pressure, ideally, the air temperature in the chamber should coincide with the temperature of its walls in the absence of any air movements. However measurements using a GLL acoustic anemometer (model АЦАТ-3М RPA "Typhoon" design, the accuracy 1 cm per second) show turbulent air flows when the chamber is in a closed state without any disturbing influences. **Figure 2** presents such measured flows.

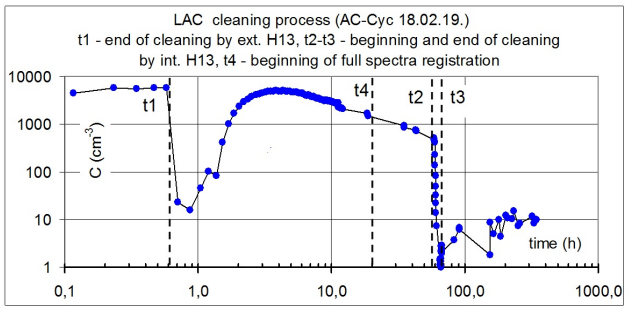

Figure 2. Vertical and horizontal wind velocity in the LAC under stationary conditions.

One can see chaotic air horizontal and vertical movements with the amplitude of several cm per sec. Because of the oversized dimensions, the temperature of the walls is inhomogeneous and induces such movements. As the result of these movements, the aerosol characteristics in horizontal directions should level, so the measurement of aerosol spectra in one point represents leveled situation for the full chamber. The aerosol characteristics of the air practically do not change after the air is mixed in the chamber using a fan.

Figure 3 shows experimental results for aerosol registration. We conducted laboratory experiment series and obtained similar results. One can conditionally divide the experiment into several stages.

The first stage is filling the LAC an outdoor air, purified by the external HEPA 13 filter and hermetically closing the LAC. This action corresponds to the time moment t_1 as shown on **Figure 3**. The stage ends at the time t_2. Each dot on the figure points to the 10-minutes cycle measurements. One can see that after cleaning the air, the particle number concentration becomes several particles per cm^3. But after that, the concentration increases and archives a maximum of $4{\cdot}10^3$ cm^{-3} approximately after 4 hours. We conclude that this is because of secondary aerosol formation due to gas-to-particle conversion. Further, the particle evolution process takes place. Finally, the particle number concentration decreases down due to Brownian coagulation. At time t_4 (approximately after 20 hours), the complete spectra registration is available.

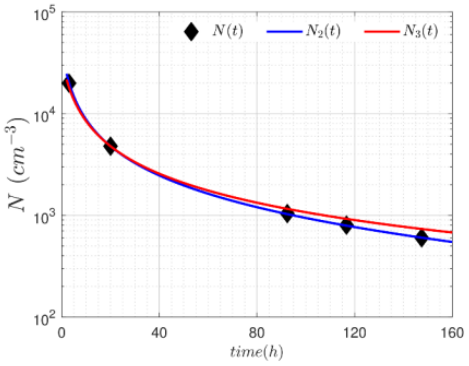

Figure 3. Particle number evolution in the air. The air was cleaned by HEPA 13 filters at two different time moments.

The second stage goes from time t_2 till t_3. Further, we second time purify the air with the internal HEPA 13 filter. Currently (approximately 2 hours), the concentration decreases to 10–20 particles per cm^3.

Figure 3 shows that after the second cleaning (time after t_3), the particle number concentration does not signifi-

cantly change and stays for a long time (more than 300 hours) at the same level of several tens particles per cm^3.

We conducted a series of such experiments, and always after the second filtration, the particle number concentration became almost zero for up to two weeks. Neither LAC walls nor turning on the equipment (including the mixing fan) influences these results.

The data on **Figure 3** leads us to conclude that after the first filtering in the LAC forming secondary aerosol from a gas component takes place. Although we cannot measure particles less than 15 nm (the lowest SMPS threshold), we assert that achieving a high concentration ($4{\cdot}10^3$) is impossible without secondary aerosol sources. These sources are some gas components in outdoor air that can form secondary aerosol particles; the authors of the paper of Hirsikko et al.[39] discovered secondary aerosols in a closed room, which seemed to have the exact nature: the specified gas components.

Since 2015, we have conducted more than 15 purposeful qualitative and quantitative experiments to study the phenomenon in the summertime and more than 8 experiments in wintertime. We turned out that the secondary aerosol formation occurred in all cases (except one case in winter). This approves the known opinion[1–4] that aerosol formation by nucleation constantly occurs in nature. However, the forming mechanism is not known yet[40].

3.2. The Observation of Aerosol Nucleation Appearance and Its Evolution at Positive Temperature

At a qualitative level, we note that autumn-summer time has a large mass concentration and narrow particle size distributions. Because of its actuality for secondary aerosol formation process understanding, we pay special attention to this period. We study in detail the synoptic cyclone situation on August, 30, 2018, when pumping in outdoor air through the external HEPA 13 filter with water content 12 g per m^3 and 20 °C temperature at 12:17 by Moscow time. The secondary aerosol formation process and further aerosol evolution we carried out during six days. **Figures 4–7** present the obtained results.

3.2.1. Evolution of the Secondary Aerosol Size Distribution

Figure 4 shows the time evolution of aerosol spectra. We mark with "external" the size distribution of outdoor aerosols with the concentration of $N_{ext} = 4{\cdot}10^3\ cm^{-3}$. Index $t = 0$ corresponds to the measurement start and coincides with the LAC filling end with the purified air with the external HEPA 13 filter. At this moment, the aerosol concentration $N_0 = 27\ cm^{-3}$. We registered particles only in separate channels. Separate marker points present the $t = 0$ curve. Following indexes refer to the points (in hours) from the chamber filling end to when measurements start.

Figure 4 shows that after 20 minutes, we observe the secondary aerosol formation with the size above the detection limit in 15 nm. Basing on the dependence, proposed in[5], we estimate the particle growth rate in the air (containing gas-precursors typical for Obninsk) injected into the LAC, as 0.7–0.8 nm h^{-1}; this value corresponds to typical estimates for mid-latitudes[5]. We detect the almost complete size distribution after three hours, and after 20 hours, there are no particles less than 20 nm. This time moment $t = 20$ hours one can consider for experimental data comparison with Equations (2) and (3). We use time moment $t = 3$ hours as qualitative data because only a tiny part of the left-hand side of size distribution is below the measured limit.

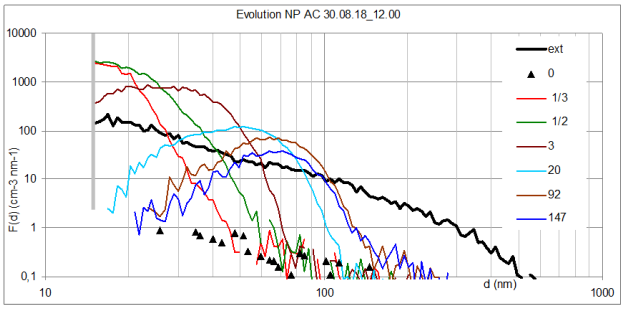

Figure 4. The secondary aerosol's formation and evolution process in the LAC after filling it with the purified with the external HEPA 13 filter outdoor air on August 30th, 2018. Curves correspond to the start time of 10 minutes cycles, measuring periods counted from the end LAC filling moment. The vertical dashed line is the threshold of the SMPS device. The word "external" means the size distribution of outdoor aerosol particles, $t = 0$ – aerosol particle size distribution measured after filling the LAC with the purifying external HEPA 13. $t = 0.3$, $t = 3$, and other – time moments (in hours) of size distribution measurement start after the LAC filling.

The analysis of aerosol particle spectra time-evolution revealed the considerable increase of mean particle size – from 30 nm to 70 nm during 150 hours of observation. The relative breadth tends to 0.25–0.29 and relative asymmetry is positive and oscillates near 2. This allows supposing gamma distribution for particle spectra evolution approximation.

3.2.2. The Particle Number Concentration Evolution Process

This section presents the number and mass concentration (**Figure 5**) related to **Figure 4**.

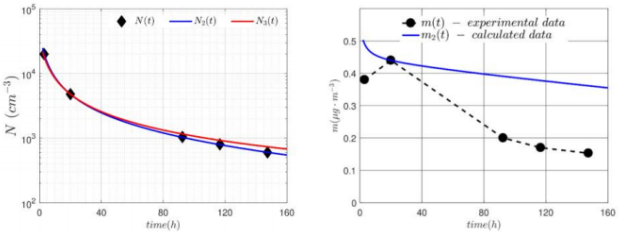

Figure 5. (**left**) Comparison of experimentally measured number concentration *N(t)* and calculated $N_2(t)$ (blue line), and $N_3(t)$ (red line) concentrations time dependencies. (**right**) experimental *m(t)* and calculated $m_2(t)$ dependences of secondary aerosol mass concentrations during their evolution process in the LAC.

Lines with marks in **Figure 5** (left) represent measured concentration in the range 15 to 1000 nm. The solid blue line represents $N_2(t)$ calculated by equation (2) with reference point $N\,(t=20) = 4200\,cm^{-3}$ (with $K = 9.05 \cdot 10^{-6}\ \left(cm^3\ per\ ours\right) \equiv 2.5 \cdot 10^{-15}(m^3\ per\ sec)$, and $D = 2.6 \cdot 10^{-3}\ \left(ours^{-1}\right) \equiv 7.2 \cdot 10^{-7}\ \left(sec^{-1}\right)$). These factors *K* and *D* we estimate with successive iterations. The discrepancy between calculated and experimentally measured values (including *t* = 3 hours) does not exceed 1.5 %. The solid red line represents dependency $N_3(t)$ obtained by Equation (3) with the same factors *K* and *N*(*t* = 20 hours) for the dependency estimation of the last term in Equation (1). The comparison between $N_2(t)$ and $N_3(t)$ shows the rate of concentration decrease increases from 1.5% after 3 hours up to 50% after 50 hours.

We calculate mass concentration from experimental data assuming spherical particle form with a density equal to 1 g per cm^3. The dashed line in **Figure 5** (right) represents these values. As seen from this figure, the mass concentration value increases by about 10 % from 3 to 20 hours. In the evolution process for $t \geq 90\ ours$, the mass concentration values decrease by about 2.5–3 times (the aerosol mass should be constant in the coagulation process). As follows from the comparison above, a significant decrease cannot be because of sedimentation, which the last term in Equation (1) defines. Figure 5 (right) represents the dependency $m_2(t)$, which considers sedimentation, calculated from the Equation (11) with $m\,(t_0 = 20\ ours) = 0.44\ \mu g\ per\ m^3$.

Neither the assumptions about the particle spherical shape nor the statement of secondary aerosol density constancy (taking into account the sedimentation) can explain the considerable decrease (about two times for the five days, *t* = 147 hours) in mass particle concentration.

We suppose that it could be because of (i) aerosol ageing resulting in its structure compaction, (ii) the overestimation of the small particle size with SMPS, or (iii) shrinking events[41].

3.2.3. Aerosol Experimental Results in the Summertime

We never vanish the left-hand side of the size distribution (below 15 nm) measuring. It means that there is a source of condensing products at least of hourly availability. One of these sources may be plant emissions. The efficiency of such a source should depend on daytime. To approve this hypothesis, we carried out experiments on aerosol evolution purified from aerosol particles air in September 2018. We filled the chamber in the evening and nighttime. The experimental results are presented in **Table 1**.

From **Table 1**, one can see that the maximum mass concentration of secondary aerosol (0.58 μg·m^{-3}) we observed during the daytime. When we sampled the air in the evening or at night, the mass concentration decreased to 0.2 μg·m^{-3} and 0.09 μg·m^{-3}, respectively. One can note the almost complete coincidence of the *ras* values in the first and last two rows of **Table 1**. The overestimation of this value for the second-row one can attribute to a short time delay. So, the values σ_c = 0.28 and ras = 2 can be considered universal asymptotic values and used in modeling the formation and evolution of secondary aerosol. The size distribution of the formed secondary aerosol is narrow. Therefore sedimentation does not influence aerosol spectra (and the gamma distribution). We assume Equation (10) as the asymptotic function for the new particle coagulation. Fixed in **Table 1**, the lowest secondary aerosol concentration at night may support the hypothesis that particles are formed from the volatile plant emissions.

3.2.4. Aerosol Experimental Results in the Wintertime

Winter aerosol differs from summer one. The first difference is the absence of a biogenic gas conversion source, which is plant emission. A similar effect was observed during the investigation of newly-formed particle formation in

Table 1. Time dependence of characteristics for outdoor aerosol and filtered aerosol in the LAC in the summer-autumn season. Date—date of air sampling, time—the local time of the chamber end filling, a—water content.

Date	Time	Outdoor Air			Air in the LAC				
		N	m	a	Δt	dm (nm)	m	σc	ras
30/08/18	12:00 LT	$3 \cdot 10^3$	7.36	12	20	52	0.44	0.30	1.9
05/09/18	18:00 LT	$20 \cdot 10^3$	15.5	12.2	16	39	0.2	0.33	2.8
06/09/18	13:00 LT	$11 \cdot 10^3$	8.6	9	20	57	0.58	0.28	1.8
18/09/18	22:30 LT	$7.3 \cdot 10^3$	4	7.9	20	33	0.09	0.25	2.4

the Antarctic [42]. New particles were detected when the air masses came from the open ocean, and there were no particles detected when the air masses came from the mainland or ice fields. The second difference is the low absolute air humidity value at negative temperatures. These low values remain after air warming in the LAC, while relative humidity decreases significantly.

We studied four situations during winter 2019 when there was solid snow in the region, gentle breeze, and stable negative temperature. **Table 2** presents the results of these studies.

The first episode on 10/01/19 with low negative temperature corresponds to the edge of an anticyclone with an isothermal temperature profile in 300 meter layer after slight snowfall. The number and mass concentration of outdoor aerosol are low. During this situation, there is no new particle formation in the LAC for 22 hours of observation. The other episodes refer to relatively low negative temperatures with a sufficiently large number and mass concentrations of aerosol. They differ in initial temperature, water content, and time on LAC filling, while characteristics of the formed in LAC particles with mass concentrations less than 0.1 μg per m^3 are almost similar.

Let us note that filling the LAC with filtered external HEPA 13 filter air takes about one hour. The filter skips particles smaller than 15 nm and gases contained in the outdoor air. These gases usually contain conversion gases that are the source of secondary particles. The new particle formation from conversion gases, their coagulation and coagulation with pre-existing in the LAC aerosol particles and conversion gases removal from the LAC, occur during the filling. Without using complex computational models of these processes, it is possible to accept the moment 20 minutes before the filling end as a start time of the aerosol evolution in the LAC. However, to avoid uncertainties arising from this, we accept the moment of the filling end as a start time.

Indeed, coagulation spectra' formation and asymptotic behavior is the subject of numerous theoretical studies [31, 32, 34]. However, for atmospheric aerosols, the theoretical study of such dependencies is complicated by uncertainty in describing the coagulation nucleus for specific situations. Until now, the modeling of such processes is a complicated process because of the influence of small chamber walls. The authors of the paper of Seipenbusch et al. [43] conducted studies of the platinum aerosol evolution with an average diameter of about 7 nm in a clean chamber of 2 m^3 volume with the presence of a simulating atmospheric aerosol. The aerosol coagulation up to about 100 nm for up to 250 minutes they got with aerosol source continuous operation due to diffusion of the aerosol onto the wall.

The fitting of analytical ratio for approximating the size distribution function is the critical aerosol characteristic in modeling both cloudy and general climatic processes. The analytical expression of aerosol spectra studies proposes two-power law four-parameter distribution [37] and the sum of three lognormal distributions [44]. To us the gamma distribution is most suitable for at least new particle formation.

4. Conclusions and Discussion

The main points of our study can be summarized as follows:

- The upgrade of the Large Aerosol Chamber (LAC) of RPA "Typhoon" with 3200 m^3 volume and HEPA 13 filters makes it possible to study gas-to-particle process formation. The main process is a new particle formation in the LAC with the purified with the external HEPA 13 filter outdoor air. This process occurs under conditions of complete darkness. (This is a novelty of our study. To our knowledge, only Dada et al. [45] tried to perform experiments in dark condi-

Table 2. Time-dependence of characteristics for outdoor aerosol and filtered aerosol in the LAC in the winter season. Date—date of air sampling, time—the local time of the chamber end filling, a—water content.

Date	Time	Outdoor Air				Air in the LAC				
		T	N	m	a	Δt	dm (nm)	m	σc	ras
10/01/19	12:00 LT	−11	$1.4{\cdot}10^3$	1.2	2.2	22	-	0.00	-	-
10/02/19	12:30 LT	−1	$7.2{\cdot}10^3$	10	4.2	20	31	0.08	0.33	2.5
14/02/19	12:00 LT	−7	$10{\cdot}10^3$	6	2.5	31	34.5	0.08	0.30	3.0
18/02/19	22:00 LT	−5	$21{\cdot}10^3$	3.8	1.9	35	42	0.095	0.34	2.9

tions.) The background concentration of ions in the air is formed by secondary galactic cosmic radiation. The next removal of these particles with the internal HEPA 13 filter results in the practically zero aerosol (27 cm^{-3}) concentration in the LAC for a very long (more than a week) period. This indicates that the conversion gases pumped in the LAC formed new particles. On the other hand, this indicates that the chamber walls and installed chamber equipment did not generate aerosol particles.

- Our experiments indicate the necessity to use the two-stage procedure for cleaning working areas, with a time gap enabling gaseous precursors to form new particles, removable by HEPA 13 filter. We found that almost full-spectrum with sizes greater than SMPS lower detection limit (d = 15 nm) disappeared (via coagulation) in 2–3 hours after filling the LAC the purified outdoor air. At the same time, the newly-formed particle concentration exceeded the value of about 104particles per cm^3 and very quickly lowered due to Brownian coagulation.
- The newly formed particle spectrum evolves (due to gas-to-particle conversion with the constant mass concentration) to the narrow "bell-shaped" spectrum with the concentration $\approx 3{\cdot}10^3$ per cm^3 about a day later. The latter evolves during the following days (five or more) due to Brownian coagulation, while its shape remains constant. The relative count standard deviation σ_c for the summer-autumn period is about 0.28, and relative asymmetry $ras \approx 2$.
- The mass concentration calculated from measured aerosol spectra (assuming that specific density equals 1 g per cm^3) varies from 0.09 to 0.6 μg per m^3 for night and daytime, respectively, during the summer-autumn period. For winter conditions, it does not exceed 0.1 μg per m^3 and does not depend on time. The decrease in plant emissions probably causes a decrease in aerosol concentration at night.

Author Contributions

All of the authors contribute equally to the paper.

Funding

The study was partially funded by RFBR and Novosibirsk region, according to research project #19 – 43 – 540009.

Data Availability Statement

Data available on request from the authors.

Acknowledgements

We are grateful to V. Yakhryushen for measuring radiation characteristics, Yu. Andreev and V. Erankov for ensuring the operation of the LAC equipment, and C. Philipchenko for help with preparing graphics.

Conflict of Interest

The authors do not declare any conflict of interest.

References

[1] Lushnikov, A.A., Zagainov, V.A., Lyubovtseva, Y.S., 2015. Mechanisms of the Formation of Nanoaerosols in the Troposphere (In Russian). Russian Journal of Physical Chemistry B. 34(10), 51–62.

[2] Whitby, K.T., 1978. The Physical Characteristic of Sulfur Aerosols. Atmos. 12, 135–159.

[3] Rozenberg, G.V., 1983. Appearance and Development

of Atmospheric Aerosol (In Russian). Izv. AN SSSR, Fiz. Atmosf. Okeana. 19(1), 21–35.

[4] Baron, P.A., Willeke, K., 2001. Aerosol measurement: principles, techniques, and applications. Second ed. Wiley-Interscience: New York. 1168 p.

[5] Kulmala, M., Vehkamäki, H., Petäjä, T., et al., 2004. Formation and Growth Rates of Ultrafine Atmospheric Particles: A Review of Observations. Journal of Aerosol Science. 35, 143–176. DOI: https://doi.org/10.1016/j.aerosci.2003.10.003

[6] Asmi, A., Wiedensohler, A., Laj, P., et al., 2011. Number size distributions and seasonality of submicron particles in Europe 2008–2009. Atmos. Chem. Phys. 11, 5505–5538.

[7] Pertti, H., Kulmala, M., 2005. Station for Measuring Ecosystem-Atmosphere Relations (SMEAR II). Boreal Environment Research. 10(5), 315–322.

[8] Dal Maso, M., Sogacheva, L., Aalto Pasi, P., et al., 2007. Aerosol Size Distribution Measurements at Four Nordic Field Stations: Identification, Analysis and Trajectory Analysis of New Particle Formation Bursts. Tellus B: Chemical and Physical Meteorology. 59(3), 350–361.

[9] Dal Maso, M., Kulmala, M., Riipinen, I., et al., 2005. Formation and Growth of Fresh Atmospheric Aerosols: Eight Years of Aerosol Size Distribution Data from SMEAR II, Hyytiälä, Finland. Boreal Environment Research. 10, 323–336.

[10] Drofa, A.S., Ivanov, V.N., Rosenfeld, D., et al., 2010. Studying an Effect of Salt Powder Seeding Used for Precipitation Enhancement from Convective Clouds. Atmos. Chem. Phys. 10, 8011–8023.

[11] Matsunaga, A., Paul, J., Ziemann, 2010. Gas-Wall Partitioning of Organic Compounds in a Teflon Film Chamber and Potential Effects on Reaction Product and Aerosol Yield Measurements. Aerosol Science and Technology. 44(10), 881–892.

[12] Zhang, X., Pandis, S.N., Seinfeld, J.H., 2012. Diffusion-Limited Versus Quasi-Equilibrium Aerosol Growth. Aerosol Science and Technology. 46(8), 874–885.

[13] Zhang, X., Schwantes, R.H., McVay, R.C., et al., 2015. Vapor Wall Deposition in Teflon Chambers. Atmos. Chem. Phys. 15, 4197–4214.

[14] Hegg, D.A., Gao, S., Hoppel, W., et al., 2001. Laboratory Studies of the Efficiency of Selected Organic Aerosols as CCN. Atmospheric Research. 58, 155–166.

[15] Yuan, Q., Zhang, Z., Wang, M., et al., 2024. Characterization of a Smog Chamber for Studying Formation of Gas-phase Products and Secondary Organic Aerosol. Journal of Environmental Sciences. 136, 570–582. DOI: https://doi.org/10.1016/j.jes.2022.12.027

[16] Huff Hartz, K.E., Rosenom, T., Ferchak, S.R., et al., 2005. Cloud Condensation Nuclei Activation of Monoterprene and Sesquiterpene Secondary Organic Aerosol. Journal of Geophysical Research. 110, D14208. DOI: https://doi.org/10.1029/2004JD005754.

[17] Wang, X., Liu, T., Bernard, F., et al., 2014. Design and Characterization of a Smog Chamber for Studying Gas-phase Chemical Mechanisms and Aerosol Formation. Atmospheric Measurement Techniques. 7, 301–313. DOI: https://doi.org/10.5194/amt-7-301-2014

[18] Chen, T., Liu, Y., Ma, Q., et al., 2019. Significant Source of Secondary Aerosol: Formation from Gasoline Evaporative Emissions in the Presence of SO2 and NH3. Atmospheric Chemistry and Physics. 19, 8063–8081. DOI: https://doi.org/10.5194/acp-19-8063-2019.

[19] Hao, L.Q., Yli-Pirilä, P., Tiitta, P., et al., 2009. New Particle Formation from the Oxidation of Direct Emissions of Pine Seedlings. Atmos. Chem. Phys. 9, 8121–8137.

[20] Virtanen, A., Joutsensaari, J., Koop, T., et al., 2010. An Amorphous Solid State of Biogenic Secondary Organic Aerosol Particles. Nature. 467(7317), 824–827.

[21] Kirkby, J., Curtius, J., Almeida, J., et al., 2011. Role of Sulphuric Acid, Ammonia and Galactic Cosmic Rays in Atmospheric Aerosol Nucleation. Nature. 476(7361), 429–433.

[22] Kirkby, J., Amorim, A., Baltensperger, U., et al., 2023. Atmospheric New Particle Formation from the CERN CLOUD Experiment. Nature GeoScience. 16, 948–957. DOI: https://doi.org/10.1038/S41561-023-01305-0

[23] Pöschl, U.T., Martin, S., Sinha, B., et al., 2010. Rainforest Aerosols as Biogenic Nuclei of Clouds and Precipitation in the Amazon. American Association for the Advancement of Science. 329(5998), 1513–1516.

[24] Lehtipalo, K., Yan, C., Dada, L., et al., 2018. Multicomponent New Particle Formation from Sulfuric Acid, Ammonia, and Biogenic Vapors. American Association for the Advancement of Science. 4(12), eaau5363.

[25] McFiggans, G., Mentel, T., Wildt, J., et al., 2019. Secondary Organic Aerosol Reduced by Mixture of Atmospheric Vapours. Nature. 565(7741), 587–593.

[26] AEROLIFE, 2000. HEPA filters. [Online] Available from: https://vozdyx.ru/page/pylevye-filtry/ (cited 8 March 2021).

[27] Gunn, R., Allee, P.A., 1954. A Three Thousand Cubic. Bulletin of the American Meteorological Society. 35(4), 180–181.

[28] Phillips, B.B., Allee, P.A., Pales, J.C., et al., 1955. An Experimental Analysis of the Effect of Air Pollution on the Conductivity and Ion Balance of the Atmosphere. Journal of Geophysical Research (1896–1977). 60(3), 289–296.

[29] Romanov, N.P., Zhukov, G.P., 2000. Thermodynamic Relations for a Vapor Chamber (In Russian). Meteorol. Gidrol. 10, 37–52.

[30] Wagner, R., Yan, C., Lehtipalo, K., et al., 2017. The Role of Ions in New Particle Formation in the CLOUD Chamber. Atmospheric Chemistry and Physics. 24(17),

15181–15197.

[31] Fuchs, N.A., 1964. The mechanics of aerosols. Translated by R. E. Daisley and Marina Fuchs; Edited by C. N. Davies. Pergamon Press: London, 1964. Pp. xiv, 408.

[32] Friedlander, S.K., 2000. Smoke, Dust, and Haze: Fundamentals of Aerosol Dynamics. Oxford University Press: New York/London. 407 p.

[33] Salimi, F., Rahman, M.M., Clifford, S., et al., 2017. Nocturnal New Particle Formation Events in Urban Environments. Atmospheric Chemistry and Physics. 17(1), 521–530.

[34] Anand, S., Mayya, Y.S., Yu, M., et al., 2012. A Numerical Study of Coagulation of Nanoparticle Aerosols Injected Continuously into a Large, Well Stirred Chamber. Journal of Aerosol Science. 52, 18–32.

[35] Smirnov, V.V., Uvarov, A.D., Savchenko, A.V., et al., 2000. Evolution of Aerosols in Large Pressurized Spaces. Journal of Engineering Physics and Thermophysics. 73(4), 832–839.

[36] Romanov, N., Erankov, V., 2013. Calculated and Experimental Regularities of Cloud Microstructure Formation and Evolution. Atmospheric and Climate Sciences. 3, 301–312.

[37] Tammet, H., Kulmala, M., 2014. Performance of Four-parameter Analytic Models of Atmospheric Aerosol Particle Size Distribution. Journal of Aerosol Science. 77, 145–157.

[38] Romanov, N., 2009. Experimental Investigation of Free (Downward) Convection Near Horizontal Cold Spots. Izvestiya, Atmospheric and Oceanic Physics. 45, 332–345.

[39] Hirsikko, A., Yli-Juuti, T., Nieminen, T., et al., 2007. Indoor and Outdoor Air Ions and Aerosol Particles in the Urban Atmosphere of Helsinki: Characteristics, Sources and Formation. Boreal Env. Res. 12, 295–310.

[40] Yermakov, A.N., Azoyan, A.E., Harutyunyan, V.O., 2019. Air Humidity Effect on the Formation of Organic Aerosol in the Atmosphere (In Russian). Optica atmosphery i okeana. 32(2), 143–146.

[41] Alonso-Blanco, E., Gomez-Moreno, F.J., Nunez, L., et al., 2015. Towards a First Classification of Aerosol Shrinkage Events. Atmos. Chem. Phys. Discuss. 15, 25231–25267. DOI: https://doi.org/10.5194/acpd-15-25231-2015.

[42] Jokinen, T., Sipilä, M., Kontkanen, J., et al., 2018. Ion-induced Sulfuric Acid–ammonia Nucleation Drives Particle Formation in Coastal Antarctica. Science Advances. 4, eaat9744.

[43] Seipenbusch, M.M., Binder, A., Kasper, G., 2008. Temporal Evolution of Nanoparticle Aerosols in Workplace Exposure. The Annals of occupational hygiene. 52, 707–716.

[44] John, W., 2011. Size Distribution Characteristics of Aerosols. In: Aerosol Measurement. John Wiley & Sons, Ltd: New Jersey, USA. pp. 41–54.

[45] Dada, L., Stolzenburg, D., Simon, M., et al., 2023. Role of Sesquiterpenes in Biogenic New Particle Formation. Science Advances. Atmospheric Science. 9, eadi5297.